Journal of Environment and Pollution ISSN: 3068-9295

PRIME OPEN ACCESS

Volume 2, Issue 1

Research Article

Date of Submission: 20 Feb, 2026
Date of Acceptance: 19 March, 2026
Date of Publication: 27 March, 2026

Effects of Strong Meteor Shower Maxima on Blood Parameters

A.V. Tertyshnikov*

Institute of Applied Geophysics, Russia

***Corresponding Author:** A.V. Tertyshnikov, Institute of Applied Geophysics, Russia.

Citation: Tertyshnikov, A. V. (2026). Effects of Strong Meteor Shower Maxima on Blood Parameters. *J Environ Pollut,* 2(1), 01-06.

Abstract

According to observations at the Russian Antarctic station Novolazarevskaya, an ordering of variations in solar ultraviolet radiation and an increase in its intensity during the maxima of strong meteor showers were detected. This effect was used in studies of blood tests from the St. Petersburg Clinical Hospital in 2000-2001. The experiment uses: the rate of erythrocyte sedimentation (ESR), the content of leukocytes and lymphocytes.

A change in the morphology of the spectral and temporal characteristics of the analyzed markers relative to the dates of strong meteor showers, with dominant cycles of 3-4 and 6-7 days, was noted.

The reasons for the interaction of solar ultraviolet radiation with meteoric dust are discussed.

Keywords: Meteor Showers, Ultraviolet Radiation, Blood Markers, Generalized Profiles, Leukocytes, Lymphocytes, Erythrocytes

Introduction

One of the mechanisms of the effect of heliogeophysical activity on the activity of society may be related to the ordering of variations in solar ultraviolet radiation. In this was shown for the maxima of strong meteor showers for hard ultraviolet [1].

Attention to the ultraviolet range is due to its comparability with the sizes of meteoric and cosmic dust particles. The change in the density of meteor dust in meteor showers, as one of the character-istics of models of meteoric matter in space, is manifested in variations in solar ultraviolet radiation.

Surface measurements of solar ultraviolet intensity were carried out at the Russian Antarctic Station Novolazarevskaya using two instruments: the UV-1 UV meter and the AvaSpec-2048 spectrophotometer [2]. The UFI-1 device allows recording the integrated power of ultraviolet radiation in the range of erythemic activity (297-330 nm). In its measuring circuit, a stream of solar radiation enters through a quartz hemispherical hood and a fluoroplastic diffuser onto a photodiode. The photodiode current is amplified by a preamp and converted by an analog-digital controller into a digital signal. The photocurrent, gain parameters and temperature inside the unit are transmitted via a USB cable to the computer input. The heater maintains the temperature inside the measuring unit within 20±2°. The fixed power level is limited to 450 W/m^2. Measurement errors of the device are up to 20% for external temperatures ± 50^{0}C.

The AvaSpec-2048 fiberoptic spectrometer allows you to diagnose the power of the ultraviolet radiation flux at several wavelengths. It was used at Novolazarevskaya, among other things, to reserve measurements with the UFI-1 device.

According to the measurement results, an increase in the recorded intensity of solar ultraviolet radiation was detected during the maxima of strong meteor showers [1]. Taking into account the modulation of variations in the intensity of solar ultraviolet radiation during strong meteor showers, the effect of a "natural germicidal lamp" can be diagnosed, for example, in characteristics and blood. The effect of solar ultraviolet radiation on blood characteristics is discusse in [3-6].

The Scheme of the Experiment

Strong meteor showers with maximum dates from were used to diagnose the effect of increases in the power of solar ultraviolet radiation on blood markers. The criterion for selecting meteor showers was the value of the zenith hour number (ZH) of at least 5 meteors per hour above a potential observer. The list of events includes streams: January 3, February 8 and 24, March 14, 7.06, 19.06, 30.07, 6.08, 13.08, 1.09, 9 September, October 21, November 17, December 7 and 14.

For the experiment, blood tests from the St. Petersburg Clinical Hospital were used from 05/28/2000 to 03/20/2001. Except in July, on public holidays and, partially, on weekends. For blood markers, the average scores from daily blood tests were used: 1) erythrocyte sedimentation rate (ESR), 2) lymphocyte content, and 3) leukocyte count. There were from five to 15 blood analyses during the day. The uncertainty in the state of health of those who took the tests determines the focus on assessing the spread of markers and their order on the generalized date of a strong meteor shower. For this purpose, the "generalized portrait" method was used in the range of ± 10 days from the dates of the maxima of strong meteor showers, and the fast Fourier transform method, taking into account the small amplitude of the expected changes in blood markers [6].

Analysis of the Results

In Figure 1.a presents estimates of the standard deviation and coefficient of variation of the average daily estimates of the erythrocyte sedimentation rate (ESR), in Figure 1.b the third and fourth moments of the distribution of the average series of ESR. The vertical arrow indicates the day with the date of the maximum of a strong meteor shower.

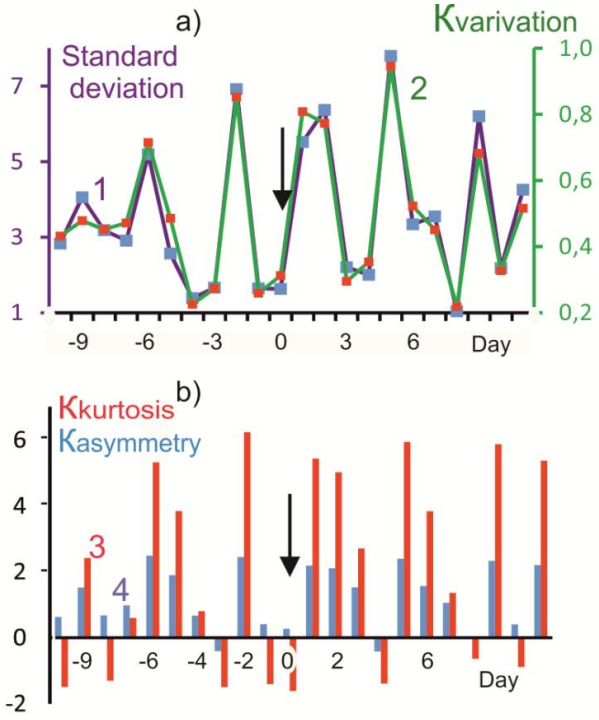

Figure 1: Variations in Average Daily Erythrocyte Sedimentation Rate Estimates

- 1(a) – estimates of the standard deviation (1) and the coefficient of variation (2),
- 1(b) – the fourth (3) and third (4) moments of the distribution of the averaged ESR series.
- The vertical arrow indicates the date of the strong meteor shower's peak.

The ESR marker allows you to assess the presence of an inflammatory process and other pathological changes in the body. The increased amplitudes of variations in the estimates obtained are noticeable in the range from -6 to +9 days from the date of the maximum of the strong meteor shower. But on the date of the maximum, with an increased level of solar ultraviolet radiation, the variations are minimal, and the marker level normalizes. The average ESR estimate on the date of the strong meteor shower was 5.2 mm/hour, with a norm of 2-10 mm/hour for men and 2-15 mm/hour for women. The ESR values on the dates -2 days and +2 days are 60% higher than on the date of the maximum of the strong meteor shower.

On the date of the maxima of strong meteor showers, the excess coefficient of the average daily ESR marker is negative (Figure 1.b), which corresponds to a uniform distribution law.
Figure 1 shows a noticeable cyclicity, which is manifested in the morphology of spectral-time amplitudograms calculated using the fast Fourier transform for a number of average daily ESR markers (Figure 2). The use of spectral-time analysis makes it possible to diagnose subtle effects in variations of natural noise.

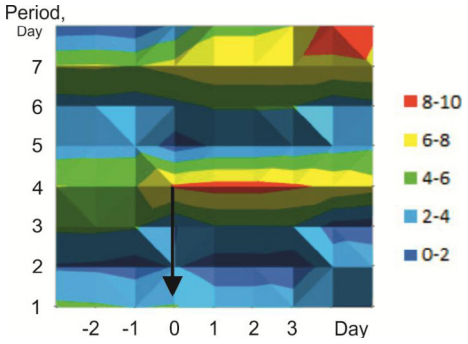

Figure 2: Spectral-Temporal Distribution of the Amplitudes of the Averaged Series of Daily Average ESR Marker Estimates. The Vertical Arrow Indicates the Date of the Strong Meteor Shower Maximum.

A 16-day sliding window was used to construct the amplitude chart. The calculated amplitude graph was assigned to its middle. The amplitude gradations are given by a color indication. The dominant cyclicity is manifested in increased amplitudes of periods of 4 and 7 days. From the date of the maximum of strong meteor showers (0-day), their amplitude increases, and decreases in the interim periods.

To compare the changes in different periods, the calculated amplitudes of each period in (Figure 2). were normalized relative to the minimum and maximum values of the amplitude of the period in the period under consideration from -3 days to + 5 days. The spectral-temporal distribution of normalized amplitudes in (Figure 2). is shown in (Figure 3), where a color indication is also used for amplitude gradations.

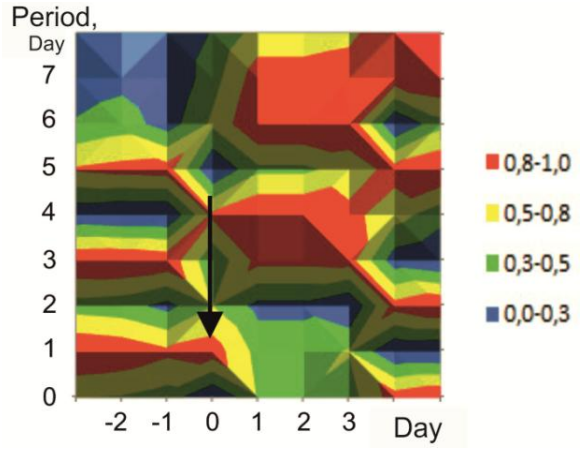

Figure 3: Distribution of Normalized Amplitude Traces for Figure 2

The vertical arrow indicates the date of the strong meteor shower's maximum.

Normalizing the amplitudes in each period improved the visibility of changes in the spectrum's morphology after the strong meteor shower's maximum, as well as the activity of the 3-4 and 6-7 day periods. The low-frequency contribution increases almost a week after the strong meteor show-er's maximum. The power of the 2-day period decreases.
The change in the average daily marker "Leukocytes" is shown in Figure 4.

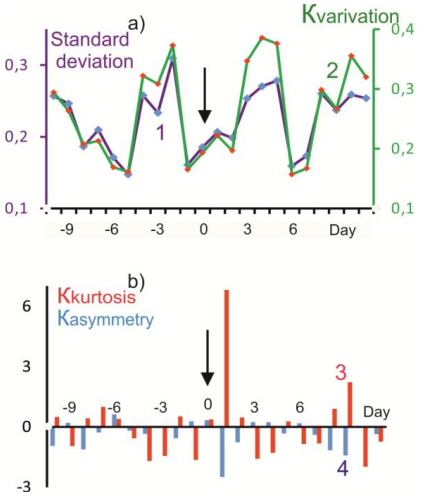

Figure 4: Variations in Average Daily Estimates of the "Leukocytes" Marker

• 1(a) – estimates of the standard deviation (1) and the coefficient of variation (2),
• 1(b) – the fourth (3) and third (4) moments of the distribution of the average series.
• The vertical arrow indicates the date of the strong meteor shower's maximum.

Leukocytes are blood cells that provide immune protection, produce antibodies, and destroy foreign agents and dead or mutated cells. Leukocytes in the blood should normally be at the level of $(0.4\text{-}0.9)\times10^{10}$/L for adults.

The level of the average daily marker "Leukocytes" is lower than the average values within ± 10 days from the date of the maximum meteor shower and increased on -3 days and on +4 days. There are also dominant periodicities of 3-4 and 7 days. Ordering of variations of average daily markers by leukocytes by estimating the kurtosis coefficient as much as one day after the date of meteor shower maxima. The signal is strong, exceeding the limits of the 95% confidence interval of the analyzed threeweek series and corresponding to the levels of the normal distribution law, which confirms the effect of ordering variations of the analyzed marker, activation of the immune system.

The changes in the average daily marker "Lymphocytes" (Figure 5) are largely similar to the estimates for leukocytes. Lymphocytes (blood cells that are involved in the formation of immune defenses) are a type of leukocytes.

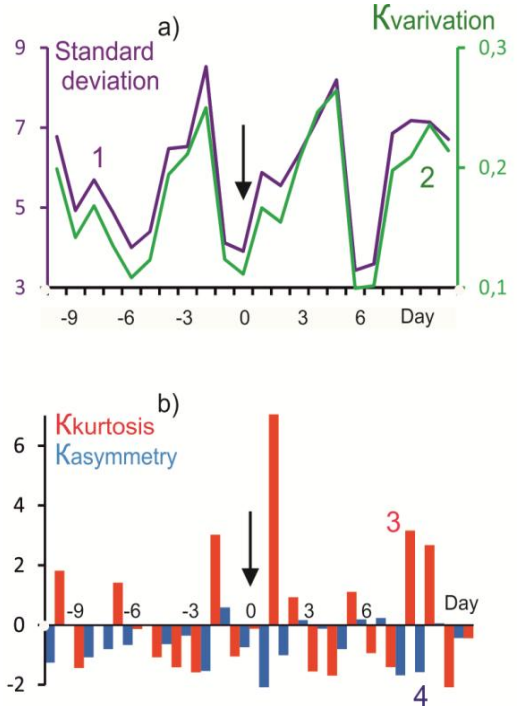

Figure 5: Variations in the Average Daily Estimates of the "Lymphocyte" Marker

1(a) – estimates of the standard deviation (1) and the coefficient of variation (2),
1(b) – the fourth (3) and third (4) moments of the distribution of the averaged series.
The vertical arrow indicates the date of the strong meteor shower maximum.

The estimate of the average daily marker "Lymphocytes" on the date of the maximum of the strong meteor shower is lower than the average values in the analyzed time period. Local maxima appear about a day later than for Leukocytes. There are also dominant periodicities of 3-4 and 7 days. A strong signal about the ordering of variations in the average daily markers of Lymphocytes is maxi-mal on the next day after the peaks of strong meteor showers, which indicates the activation of the immune system. The main task of Lymphocytes is to recognize and destroy agents foreign to the body primarily pathogens of infectious diseases and their own damaged cells.

Discussion

The time correspondence of the weak impact of variations in meteor shower density on the upper atmosphere with changes in blood markers necessitates the search for possible mechanisms of in-teraction. These may include changes in atmospheric conductivity due to meteor dust, an increase in the influx of solar ultraviolet radiation into the maximum meteor shower, the influence of solar ultraviolet radiation on pathogenic processes, and variations in the density of the meteor shower in the solar ultraviolet stream.

The models of the distribution of meteoric matter do not take into account variations in the density of the meteor shower, including in the upper atmosphere. The first model is designed to calculate the spatial distribution of meteoric matter in the ecliptic plane with a particle mass of 10^{-6} ...10^{2} g at a distance from the Earth's surface up to ~1000000

km and meteoroids with a mass of 10^{-9} ... 10^{-6} g at a distance of 200-1000 km. Moreover, the velocities of meteor bodies weighing up to 10^{-6} g relative to the Earth are assumed to be 20 km/s [7-9]. In the further development of models for the dis-tribution of meteoric matter, priorities were given to space debris models which require special consideration of dust from the burning of Starlink satellites. The distribution of meteoric dust from the Earth's surface to the exosphere, in the mesosphere and stratosphere remains unexplored [10].

NASA and ESA regularly update working versions of existing meteoroid matter models that are used in spacecraft design and planning of various space missions. However, even in these models, the range up to 0.1 astronomical units from the Earth remains ignored although meteor dust particles are selected due to the ballistic deceleration of meteor dust particles: with a decrease in the mass and size of dust particles, their ballistic coefficient increases, characterizing deceleration [11,12]. In this case, the aerodynamic accelerations for a dust particle are two orders of magnitude greater than for a micrometeoroid of a meteor shower with a size, for example, an order of magnitude larger and with the same amount of static stability margin. Due to this, large fragments of the meteor shower break out ahead, since with a decrease in the size of dust particles and the same density of dust and micrometeoroids, their ballistic coefficient is inversely proportional to the cube of the diameter, and the area of the module is proportional to the square of these dimensions. As the mass of dust particles increases, the sensitivity of their deceleration to variations in the density of the upper atmosphere decreases. Micrometeoroids smaller than the critical one (~100 micrometers) slow down above 100 km slowly enough to emit frictional energy without melting. Therefore, they can reach the earth's surface.

Selection of meteor shower fractions by aerodynamic braking contributes to variations in the observed zenith optical density of meteor showers. For larger fractions that outpace the arrival of fine dust, the transparency of the atmosphere for solar ultraviolet radiation will be higher on the date of the maximum meteor shower. In addition, the long axis of the dust grains unfolds perpendicular to the lines of force of the weak magnetic field. The resulting dusty anisotropy of conductivity in the Earth's electric field contributes to the polarization of transmitted light and diffraction of solar ultraviolet radiation.

Variations in the settling density of meteor dust are also influenced by the thermodynamics of the atmosphere. The dominant periodicity of 6-7 days in variations of the daily ESR marker corresponds to the time delay required to reach the maximum meteor flow from the height of the turbopause at a speed of about 3 km/day to the heights of the mesopause, where meteor dust can accumulate due to thermodynamic gradients of the atmosphere. The accumulation of settling meteor dust at the heights of the mesopause is manifested in variations in the passing ultraviolet radiation, affecting the mode of the "natural germicidal lamp".

Below the mesopause, a layer of anomalous thermodynamic gradients is located at stratopause heights, in the ozonosphere, at the velopause level. These layers also have conditions for the accumulation of meteoric dust. But below 20 km and the Young's layer, terrestrial and cosmic dust are actively mixed.

The effect of meteor dust on the Chapman cycle during the formation of ozone molecules and on the ozone sphere requires further research, since meteor showers create unique conditions for variations in the solar hard ultraviolet. For an example of this effect, Figure 6 shows "generalized portraits" of the kurtosis coefficients and the symmetry of satellite measurements at a wavelength of 121.6 nm for 2008-2023. The arrow indicates the date of the maxima of strong meteor showers on December 14 (a) and August 13 (b).

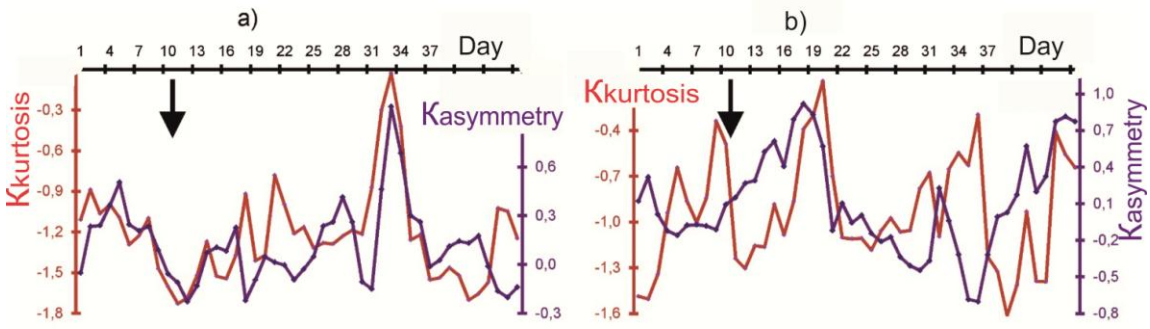

Figure 6: "Generalized Portraits" of the Kurtosis and Asymmetry Coefficients of Satellite Measurements of Extreme Ultraviolet Radiation at a Wavelength of 121.6 nm for 2008-2023. for the Date (Arrow) of the Maxima of Strong Meteor Showers: December 14 (a) and August 13 (b)

The 11th day of the timeline falls on the indicated dates of the maximum meteor showers. The 33rd day of the scale in (Figure 6.a) correspond to January 6, which is almost the beginning of Christmas frosts and the arrival of meteor dust at the stratopause level, where its spatial distribution is heterogeneous. This effect will manifest itself in the thermodynamics and morphology of the ozone sphere and below with a delay of several days. The anomalous burst on fragment 6a may be due to the coincidence of the December meteor shower complex.

For the August Perseids in (Figure 6.b), the coefficient emissions occur on August 22 and the first decade of September. By August 22, meteor dust overcomes the mesopause and its illumination by solar ultraviolet radiation reaching the ozonosphere in the range of 315-400 nm "depresses" the thermodynamics of the ozonosphere with subsequent phenomenological effects by the autumn equinox.

The considered effects will inevitably manifest themselves in blood markers.

Conclusions

As a result of statistical processing of blood tests from the St. Petersburg Clinical Hospital, changes have been identified that correspond in time to the dates of strong meteor showers and an increase in incoming solar ultraviolet radiation.

In the dynamics of ESR estimates characterizing the activity of inflammatory processes, dominant cycles with periods of 3-4 and 6-7 days were noted.

The content of leukocytes and lymphocytes revealed similar effects with minima on the dates of meteor shower maxima, dominant periodicities and strong signals of activation of immune system processes after the maxima of strong meteor showers.

The deposition of cosmic and meteoric dust into the ozonosphere is of interest to astrobiology.

Acknowledgments

The author thanks Sergei Nikolaevich Shapovalov (St. Petersburg) for providing measurement data and consultations, and Igor Olegovich Ryabinin (St. Petersburg) for consultations on instruments and measurements.

Reference

1. Tertyshnikov, A. V. (2025). Variations in F 10.7 by New Dates of Maximum Meteor Streams. Solar System Research, 59(5), 56.
2. Ryabinin I.O. UV radiation meter, spectroradiometer, spectrophotometer.
3. Shapovalov, S. N. (2021). Dependence of UVB-UVA Solar Radiation in the 280–400 nm Range on Changes in the Total Magnetic Field of the Sun. Russian Meteorology and Hydrology, 46(3), 212-216.
4. Varakin Yu.Ya., Ionova V.G., Gornostaeva G.V., Sazanova E.A., Sergienko N.P., Tedoradze R.V (2011). "The Effect of Heliogeophysical Disturbances on Hemorheological Parameters in Healthy Individuals" // Zemsky Vrach. 2011, №. 2. pp. 21-24.
5. Komarov F.I., Breus T.K., Rapoport S.I. et al. (1994). Medical and biological effects of solar activity // Bulletin of the Russian Academy of Medical Sciences. 1994. № 11. Pp. 37-49.
6. Tertyshnikov A.V. (1999). Seismo-ozone effects and the problem of earthquake prediction. – St. Petersburg: A.F. Mozhaisky VIKU, 1999. 197 p.
7. GOST 25645.128-85. (1985). "Meteoric substance. Spatial distribution model". Moscow: Publishing House of Standards, 1985. 24 p.
8. Grün, E., Zook, H. A., Fechtig, H., & Giese, R. H. (1985). Collisional balance of the meteoritic complex. Icarus, 62(2), 244-272.
9. Mironov, V. V., & Tolkach, M. A. (2017). Models of meteoroid environment in near Earth space and determination of the meteoroid flux density. Kosmicheskaya tekhnika i tekhnologii, 49-62.
10. GOST 25645.167- (2005). Space environment (natural and artificial). Model of spatiotemporal distribution of flux density of technogenic substance in outer space. Moscow: Standartinform, 2005. 36 p.
11. Wiegert, P., Vaubaillon, J., & Campbell-Brown, M. (2009). A dynamical model of the sporadic meteoroid complex. Icarus, 201(1), 295-310.
12. Tertyshnikov, A. V. (2020). Capabilities for Probing Upper Atmosphere Density Variations and Seismic-Orbital Effects Using Small-Size Spacecraft. 306.